Use of calcined layered double hydroxide [Zn$_2$-Al-CO$_3$] for removal of textile dye acid green 1 from wastewater: kinetic, equilibrium, comparative, and recycling studies

El Hassane MOURID[1] , **Mohamed LAKRAIMI**[1,*], **Souad EL ABRIDI**[1], **Lhaj BENAZIZ**[1],
ELKHATTABI[2], **Moha BERRAHO**[2]

[1]Physical Chemistry of Materials Team, Cadi Ayyad University, Marrakech, Morocco
[2]Laboratory of Biomolecular Chemistry, Cadi Ayyad University, Marrakech, Morocco

Abstract: In the present study, calcined layered double hydroxides (CLDHs) were obtained by heating [Zn$_2$-Al-CO$_3$] at 500 °C. The adsorption of the textile dye acid green 1 (AG1) by CLDH was carried out at different pH levels, adsorbent–adsorbate contact times, and AG1/CLDH mass ratios. Equilibrium at room temperature was reached after 24 h, which was confirmed by the kinetic modeling of the experimental data by the pseudo-second-order model. The adsorption is described by a Langmuir-type isotherm. The comparative study of adsorption isotherms in calcined and uncalcined phases reveals that the former could be a good candidate for trapping such pollutants. After removal of AG1, characterization of the CLDH solids by X-ray diffraction and infrared spectroscopy showed that the adsorption is also enhanced by reconstruction of a hydrotalcite matrix intercalated by AG1. The removal of AG1 by CLDH gave satisfactory results. Under optimum conditions, the retention is total when mass ratio AG1/CLDH is between 0.58 and 0.75. The material can be recycled by a series of anion exchange reactions and its retention capacity reaches 833.33 mg/g. This retention capacity was only reduced by 10% after the fifth recycling cycle.

Key words: Calcined layered double hydroxide, AG1 textile dye, adsorption, intercalation, reconstruction, recycling

1. Introduction

Current developments in various industries directly or indirectly influence the environment, specifically the soil, air, and water. The rapid growth of industries has a detrimental effect on human health and ecology through the emission of effluents directly without prior treatment. Dyes are a major source of pollution; they are used in many industrial sectors such as textiles, paper, pharmaceuticals, food, and cosmetics.[1] Dyes are known for their environmental toxicity.[2] No one can deny that the textile industries are a very big consumer of water and synthetic dyes, which constitute a real industry of modern chemistry. Synthetic dyes are distinguished by the chromophoric groups they contain (azo, anthraquinone, etc.), or by the field of application (reagent, dispersed, etc.). Due to their massive use and demand, global production of these dyes is estimated at 800,000 t/year, of which about 140,000 t/year are removed during tissue production.[3]

In Morocco, the textile industry represents about 31% of all national industries whose reactive dyes are widely used in relation to other dyes; they are specifically distinguished for the dyeing of wool and nylon. In the textile industry, about 1000 L of water is used per 1000 kg of clothes processed in dyeing.[4] After their use, these

---

*Correspondence: mlakraimi@yahoo.fr

dyes are always present in wastewater in low amounts and are highly visible and undesirable. Their presence endangers living organisms.[5] Various processing methods, such as physical, chemical, and biological treatment of effluents, are used for the elimination of the dyes from wastewater. However, the majority of these methods are expensive and generate large quantities of sludge,[6] so adsorption is widely used to remove dyestuffs from wastewater.[7,8] Due to the biological and chemical stability of these dyes, adsorption on adsorbent material is considered an alternative and effective method for removing dyes and other pollutants that exist in wastewater. In recent years, adsorbent materials such as smectite,[9] activated carbon,[10] and kaolinite[11] have been used to remove different types of dyes according to their affinity in relation to these materials. Other authors have used chitosan as an adsorbent of dyes[12] or coupled with clays.

The objective of this research is to study the elimination efficiency of the textile dye acid green 1 (AG1) by a calcined layered double hydroxide (CLDH), as well as to optimize the various parameters governing the adsorption such as pH, contact time, initial dye concentration, and AG1/CLDH mass ratio. These materials have great potential for removing effluent pollutants such as dyes and herbicides,[13] are relatively low-cost, are recyclable, and do not generate sludge.

The layered double hydroxides (LDHs) can be represented by the following general formula:[14]

$$[M_{1-x}^{2+} M_x^{3+}(OH)_2](A^{n-})_{x/n}.mH_2O,$$
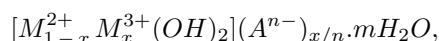
where M^{2+} is a divalent cation, M^{3+} a trivalent cation, A^{n-} an interlayer anion, and x the $M^{II}/(M^{II}+ M^{III})$ ratio.

After rehydration, the mixed oxides resulting from the calcination of LDH at 500 °C have already shown their ability to reconstruct an original layer structure because they have a so-called memory effect.[15] This property of reconstructing new LDH phases, which is favored by the adsorption of various anions, places them among the good adsorbents to remove toxic anions from contaminated water.[14−18] In this context, we have studied the removal of the AG1 textile dye from an aqueous solution using calcined LDH [Zn_2-Al-CO_3]. The localization of AG1 in the interlamellar space and/or on the outer surfaces of the reconstructed LDH phase is studied by X-ray diffraction (XRD), infrared spectroscopy (IR), and scanning electron microscopy (SEM).

2. Results and discussion

2.1. Characterization of [Zn_2-Al-CO_3]

2.1.1. XRD

Characterization of [Zn_2-Al-CO_3] by XRD (Figure 1) showed that the phase corresponds to a pure LDH.[19] The solid consists of a well-crystallized single phase with large constituting crystallites. The lattice parameters refined on the hexagonal setting with a rhombohedral symmetry (space group: R?[U+F8E5]3m) and the experimental metal ratios are given in Table 1.

Table 1. Experimental [Zn]/[Al] ratio in the solid and its cell parameters.

[Zn]/[Al]$_{th}$	[Zn]/[Al]$_{exp}$	a (nm)	c (nm)	d (nm)
2.00	1.99	0.306	2.292	0.764

2.1.2. IR

The IR spectrum of the intercalated phase by carbonate anions (Figure 2) shows bands at 3470 and 1630 cm^{-1} corresponding respectively to the valence vibrations of hydroxyl groups of the brucite layers (ν_{OH}) and deformation vibration of interlayer water molecules (δ_{H2O}).
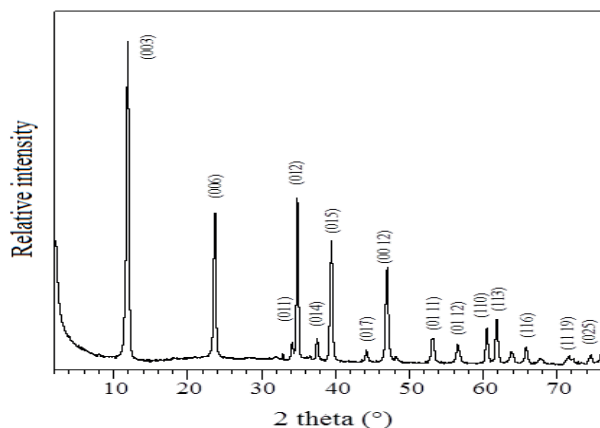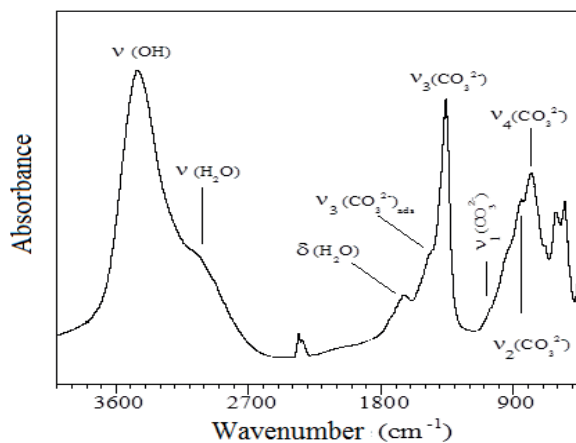

Figure 1. XRD pattern of [Zn$_2$-Al-CO$_3$] LDH.

Figure 2. IR spectra of [Zn$_2$-Al-CO$_3$].

It is important to note the presence of a shoulder at 3040 cm^{-1} in this spectrum. Many authors have shown that this shoulder corresponds to a hydroxyl ion-stretching vibration associated with carbonate anions by hydrogen bonds in pyroaurite type minerals.[20−22]

The so-called free carbonate anion belongs to the symmetry group D$_{3h}$ and only ν_2, ν_3, and ν_4 vibrations, respectively, at 879, 1430, and 706 cm^{-1} are active in infrared in a reference compound such as CaCO$_3$.[23,24]

However, the frequency of the ν_3 vibration on the spectrum of [Zn$_2$-Al-CO$_3$] is lowered to a few tens of cm^{-1} with respect to the observed frequencies of CaCO$_3$ (1430 cm^{-1}). We can deduce that the carbonate anions do not have the same environment in both materials.

In [Zn$_2$-Al-CO$_3$], the shoulder at 1550 cm^{-1} and the appearance in the vicinity of the 1150 cm^{-1} band of ν_1 show that some carbonate anions may exist in a different symmetry, suggesting that they are not inserted between the sheets but rather adsorbed on the surface of monocrystallites.[25]

2.1.3. SEM

The SEM image corresponding to the [Zn$_2$-Al-CO$_3$] phase is shown in Figure 3. The lamellar structure is well highlighted by the presence of crystallites, which are distributed more homogeneously.

2.2. Adsorption equilibrium

Preliminary adsorption experiments were conducted to determine the optimal conditions for the retention of AG1 on CLDH regarding the pH value, contact time (t_c), and the mass ratio of adsorbate/adsorbent.

2.2.1. Effect of pH

Generally, pH is considered an important parameter that controls adsorption at water–adsorbent interfaces. On one hand, it fixes the degree of ionization of the acid or basic functional groups of the adsorbates and controls the speciation of the solution and, on the other hand, it modifies the surface charge of the support, such as layered double hydroxides. Keeping this in mind, the adsorption of AG1 on CLDH was studied at different pH values ranging from 5 to 10 (Figure 4). Dye adsorption on CLDH is at its maximum at a pH between 6 and 7. The smaller adsorbed amount observed at pH 5 may be attributed to a partial dissolution of the mineral matrix by acidic hydrolysis.[26−28]

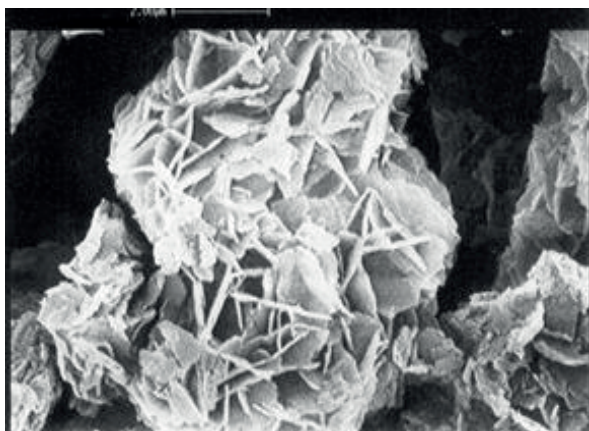

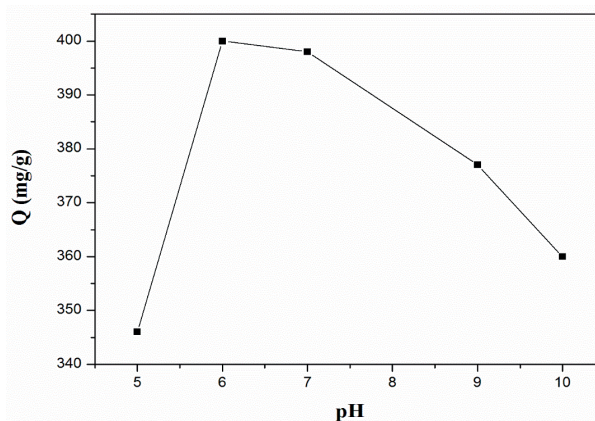**Figure 3**. SEM photograph of $[Zn_2\text{-Al-CO}_3]$.

Figure 4. Amount of AG1 retained by CLDH at different pH values ($m_{CLDH} = 50$ mg, $C_i = 200$ mg/L, $t_c = 24$ h).

The decrease of the adsorption observed when the pH increases can be explained by a complicity imposed by the carbonate anions, which have a high affinity to the LDH materials.[29] This phenomenon takes place despite the precautions taken during the preparation of the solid adsorbent and the study of the adsorption when the pH value is high.

Thereafter, all experiments were carried out at pH between 6 and 7, knowing that at these values, the AG1 dye has an anionic form in aqueous solution.

2.2.2. Effect of contact time

The amount of AG1 adsorbed as a function of contact time is shown in Figure 5. The kinetic study shows that the adsorption equilibrium state is reached after a contact time of 24 h since no change in the adsorbed amount is detected afterwards. Similar behavior was obtained for pesticide 2,4-D with calcined $[Zn_2\text{-Al-CO}_3]$ at 500 °C.[30]

To be sure that the equilibrium state is reached for higher concentrations, an AG1-CLDH contact time of 24 h was applied in the retention experiments.

2.3. Adsorption kinetics

2.3.1. Pseudo-first and pseudo-second order

For the examination of the controlling mechanisms of adsorption process, such as chemical reaction, diffusion control, and mass transfer, several kinetics models are used to test the experimental data. In this study, two
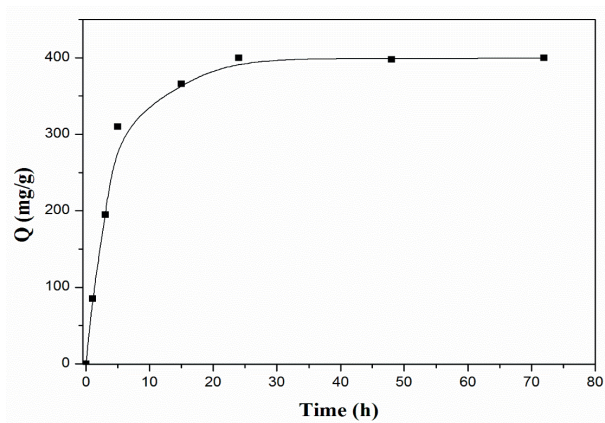
Figure 5. Amount of AG1 ($C_i = 200$ mg/L) sorbed by 50 mg of CLDH versus contact time.

kinetic models were used to fit the experimental data of AG1 dye adsorption onto CLDH:

$\ln (Q_e - Q_t) = \ln Q_e - k_1 t$: pseudo-first order.[31]

$t/Q_t = 1/(k_2 Q_e^2) + (1/Q_e)t$: pseudo-second order.[32]

Here, Q_e (mg/g) and Q_t (mg/g) are the amount of AG1 adsorbed at equilibrium and at time t (h), respectively. k_1 and k_2 are the rate constants of the pseudo-first- and pseudo-second-order models of adsorption.

The resulting linearizations of both models are summarized in Table 2.

Table 2. Adsorption kinetics describing the order and correlation coefficients for retention of AG1 by CLDH ($C_i = 200$ mg/L, $m_{CLDH} = 50$ mg).

Pseudo-first order				
Equation	k_1 (h^{-1})	$Q_{e\,th}$ (mg/g)	$Q_{e\,\exp}$ (mg/g)	R^2
$\ln(Q_e - Q_t) = -0.0595 \times t + 3.7251$	0.0595	41.47	400.00	0.3721
Pseudo-second order				
Equation	k_2 (g/mg/h)	$Q_{e\,th}$ (mg/g)	$Q_{e\,\exp}$ (mg/g)	R^2
$t/Q_t = 0.0024 \times t + 0.0061$	0.0009	416.67	400.00	0.9987

The correlation coefficient of the pseudo-second-order equation is better than that of the pseudo-first-order equation. This is also true if we compare theoretical and experimental values of Q_e. It can be said that the AG1 retention kinetics by CLDH are in good agreement with the model of the pseudo-second order.

2.3.2. Intraparticle diffusion

To investigate the contribution of intraparticle behavior to the adsorption process, the rate constant for intraparticle diffusion can be calculated from the following equation:[33,34]

$$Q_t = k_{ip} t^{1/2} + C,$$

where k_{ip} is the intraparticle diffusion rate constant (mg/g) and C is the vertical axis intercept. If the plot of Q_t against $t^{1/2}$ is linear, the adsorption process is deemed to have been determined by the intraparticle diffusion step.

Indeed, in this work, these lines correspond to the existence of the external diffusion process (external surface adsorption), followed by intraparticle diffusion and finally a slow diffusion of the adsorbate to the micropores of the adsorbent.[35,36]

The intraparticle diffusion model of AG1 adsorption onto CLDH is shown in Figure 6. It may be noted that the diffusion mechanism of the adsorption system is described by three distinct regions instead of one linear over the entire domain, implying that the process has more than one step. The intermediate step is evident.
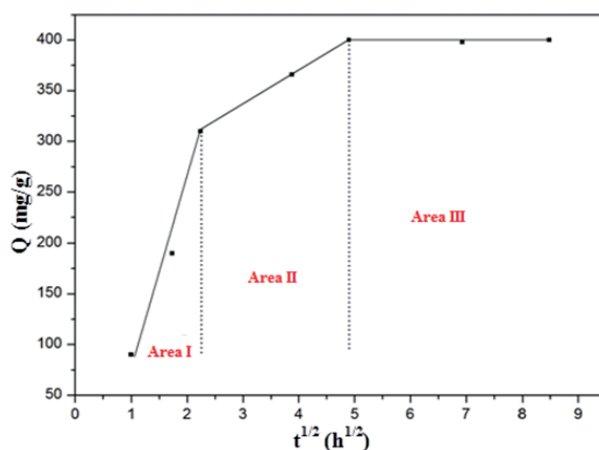

Figure 6. Intraparticle diffusion kinetic for adsorption of AG1 ions on CLDH.

For intraparticle diffusion, most curves show three linearities:[37−39]

- Area I: Adsorption on the surface.
- Area II: intraparticle diffusion (intercalation between the layers of the reconstructed LDH phase).
- Area III: Corresponds to the saturation (steady state).

The constants for intraparticle diffusion are listed in Table 3.

Table 3. Rate constants and correlation coefficients for intraparticle diffusion.

Area I Equation: $Q_t = 175 \times t^{1/2} - 93.146$		
k_{1p} (mg/g/h$^{1/2}$)	C_1 (mg/g)	R^2
175	−93.146	0.9751
Area II Equation: $Q_t = 33,836 \times t^{1/2} + 234.51$		
k_{2p} (mg/g/h$^{1/2}$)	C_2 (mg/g)	R^2
33.836	234.51	0.9999
Area III Equation: $Q_t = 0.005 \times t^{1/2} + 399.89$		
k_{3p} (mg/g/h$^{1/2}$)	C_3 (mg/g)	R^2
0.005	399.89	0.9957

2.4. Adsorption isotherms

Figure 7 displays the retention isotherms of AG1 onto 50, 60, and 80 mg of CLDH. The AG1 adsorption isotherms on calcined [Zn$_2$-Al-CO$_3$] can be considered clearly as H-type, indicating that the interaction of

sorbate–sorbent is much stronger than solvent–sorbent at the adsorption sites (high affinity between AG1 and CLDH). Isotherms with this profile are typical of systems where the functional adsorbate is strongly attracted by the adsorbent, mostly by ion–ion interaction, which tends to reach a saturation value given by a nearly isotherm plateau. These results again suggest that AG1 anions are preferentially removed.
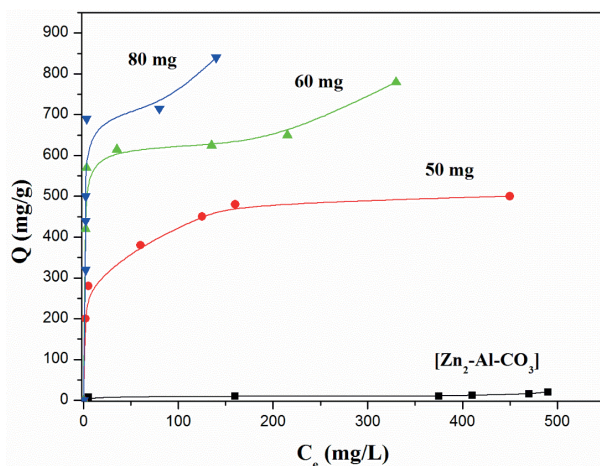

Figure 7. Adsorption isotherms for AG1 determined with three different doses of CLDH (50, 60, and 80 mg) and uncalcined LDH [Zn_2-Al-CO_3].

We note that the retention of AG1 is proportional to the mass of CLDH and then these isotherms are of the Langmuir type. This proves that the retention of the pollutant is achieved by reconstruction of LDH phases intercalated by AG1. Retention by uncalcined [Zn_2-Al-CO_3] is not significant because of the greater affinity of carbonates for LDH.

The data for the adsorption of AG1 have been processed in accordance with the linear forms of Freundlich and Langmuir isotherms equations:[40]

Freundlich: $\log (Q_e) = \log (K_f) + 1/n \, \log (C_e)$.

Langmuir: $C_e/Q = (1/KQ_m) + C_e/Q_m$.

Q is the quantity of AG1 retained by the unit mass of CLDH (mg/g); Q_m, is the maximum quantity of AG1 retained by the unit mass of CLDH (mg/g); C_e is the equilibrium concentration of AG1 (mg/L), and K is the affinity constant of AG1 for CLDH (L/mg). K_f (mg/g) is a function of energy of adsorption and temperature and is a measure of adsorptive capacity, and $1/n$ determines the intensity of adsorption.

A linear relationship was observed among the plotted parameters, which indicates the applicability of the Langmuir equation. The sorption parameters obtained are summarized in Table 4.

Table 4. Langmuir and Freundlich isotherms model constants and correlation coefficients for retention of AG1 by CLDH.

m_{CLDH} (mg)	Langmuir isotherm			Freundlich isotherm		
	Q_m (mg/g)	K (L/mg)	R^2	K_f (mg/g)	n	R^2
50	500.00	0.131	0.998	9.877	6.006	0.958
60	769.23	0.134	0.985	14.225	12.594	0.741
80	833.33	0.461	0.993	13.728	7.257	0.589

Note that the K values are relatively comparable, which lets us state that the type of interaction between the adsorbed molecule AG1 and the CLDH surface is the same regardless of the mass of CLDH used. However, the values of Q_m vary depending on the mass.

These results are confirmed by other analytical techniques (XRD, IR, and SEM) for products obtained after retention.

2.5. Study by XRD

The solid compounds collected after contact with the solution of the dye AG1 for different mass ratios of AG1/CLDH were analyzed by XRD. The spectra of the phases obtained are shown in Figure 8.
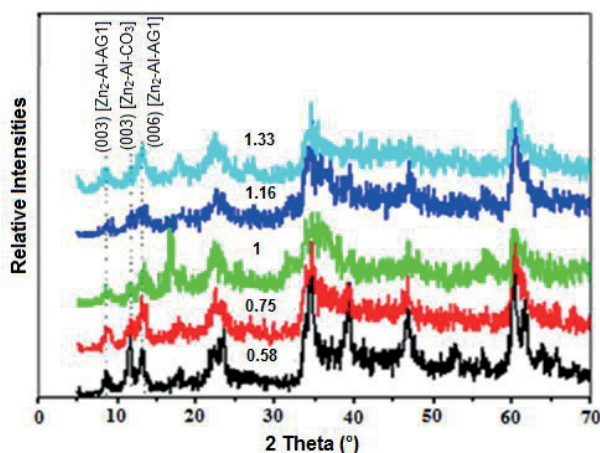

Figure 8. XRD patterns of the phases obtained after retention of AG1 at different mass ratios m_{AG1}/m_{CLDH}.

The XRD patterns obtained after retention with varying amounts of AG1 indicate that these phases correspond to hydrotalcite-like materials. However, the crystallinity of reconstructed phases is lowered; this is detected by peak broadening and the decrease of their intensities. For mass ratios of AG1/CLDH lower than or equal to 1.16, there is the reconstruction of two phases, one intercalated by carbonates whose interlamellar distance is 0.764 nm and the other by the AG1 dye with $d = 0.98$ nm. One can argue that there is competition between the dye anions and carbonate anions for the reconstructed LDH sheets. Contamination from carbonates during the LDH rehydration experiments was inevitable and probably the amount of AG1 was not sufficient to limit it.

On the other hand, when the mass ratio of AG1/CLDH is greater than or equal to 1.33, there is disappearance of the line (003) characteristic of the phase intercalated by carbonates. That is to say that we are witnessing the reconstruction of a single phase intercalated by AG1 dye. The amount of dye in this case is probably sufficient to minimize the intercalation of carbonates.

We can conclude that for these domains of mass ratios, the AG1 retention is done in two ways: adsorption on the surface and intercalation between the layers of the reconstructed matrix.

The removal of textile dye in anionic form by CLDH gave satisfactory results. Under optimum conditions, the retention is total (100%) when the mass ratio of AG1/CLDH is between 0.58 and 0.75. Retention capacity reaches 833.33 mg/g.

The lattice parameters for that phase intercalated by AG1 [Zn_2-Al-AG1] are $a = 0.306$ nm, $c = 2.94$ nm, and interlamellar distance $d = 0.98$ nm.

This value suggests a horizontal disposition of AG1 anion in the interlayer space (parallel to the planes of the layers). The adoption of a horizontal orientation, parallel to the LDH sheets for simple or large organic molecules, has been proposed by other authors as porphyrins with $d = 1.17$ nm,[41] oxalates with $d = 0.778$ nm, oxalates aluminum with $d = 0.99$ nm, hydroxyterephthalates with $d = 1.08$ nm,[42,43] or methyl orange with $d = 0.856$ nm.[44]

2.6. Study by IR

The results obtained by IR for [Zn_2-Al-AG1] ($m_{AG1}/m_{CLDH} = 1.33$) are in agreement with those of XRD; they clearly confirm the characteristic bands of AG1 (Figure 9).

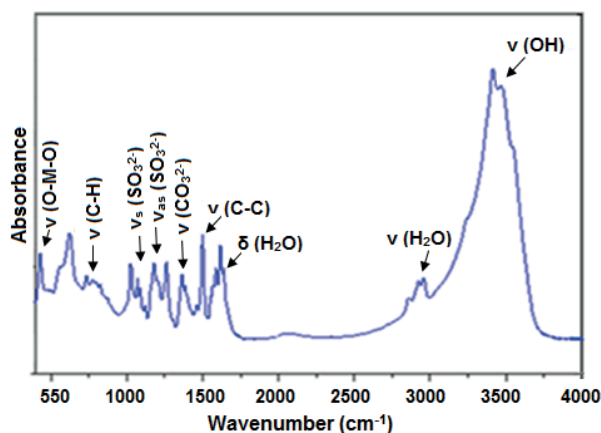**Figure 9**. IR spectrum of [Zn_2-Al-AG1] phase obtained after retention of AG1 at mass ratio $m_{AG1}/m_{CLDH} = 1.33$.

The broad band at 3400 cm^{-1} corresponds to OH-stretching vibrations. The band centered at 1628 cm^{-1} corresponds to the deformation vibrations of the water molecules inserted between the LDH sheets. These bands reveal the presence of hydroxyl ions arising from the brucite layers. The band at 1360 cm^{-1} is attributed to the characteristic vibrations of carbonate contamination.

The characteristic vibrations of AG1 located around 1500 cm^{-1} correspond to the bonds of C=C vibrations of the benzene ring.

In the region between 1100 and 1260 cm^{-1}, we observe symmetric and asymmetric vibration sulfonate groups.[45] This shows that the AG1 retention is by interaction between sulfonate groups of the intercalated dye and the hydroxyl groups of the reconstructed layers (LDH phase).

Bands between 700 and 800 cm^{-1} correspond to the deformation vibrations (C-H) outside the benzene cycles.

Bands at 1640, 1300, and 1188 cm^{-1}, respectively, correspond to the vibrations of C=O, C-O, and C-N.

We also note that the characteristic vibrations of LDH sheets (around 430 and 638 cm^{-1}) were observed with apparent intensities.[26]

2.7. Analysis by SEM

SEM of calcined [Zn_2-Al-CO$_3$] at 500 °C and that of [Zn_2-Al-AG1] was carried out at a magnification of 10,000×. The sample shows aggregates of crystallites formed perpendicular to the image plane (Figure 10).

For the calcined matrix (CLDH), it presents relatively smaller particles and nonuniformity due to the destruction of the lamellar character of our material. We are also witnessing the emergence of a mottled appearance of some crystallites or even some agglomerates. These can correspond to the segregation of mixed oxides.[27,41]
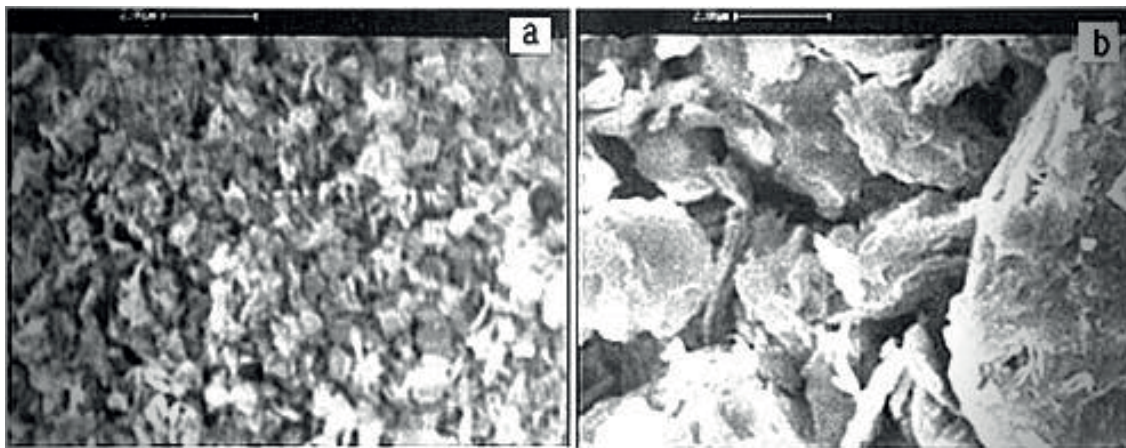

Figure 10. SEM photographs of calcined LDH [Zn_2-Al-CO_3] (a) and reconstructed phase [Zn_2-Al-AG1] (b).

The lamellar character of the intercalated compound by the dye [Zn_2-Al-AG1] appears obvious, which shows a reconstruction of a hydrotalcite phase. The sample shows aggregates consisting of crystallites resulting from the superposition of layers. These crystallites are of different sizes and may be up to 2 μm. The crystalline organization is relatively low compared to that of the uncalcined matrix [Zn_2-Al-CO_3] (Figure 3). This result is confirmed by XRD patterns of the two compounds.

2.8. Comparative study

The superficially active substances in industrially used water cause major environmental problems. To this end, several research projects are part of the development of substances that have a high potential for adsorption of these pollutants. Several studies have shown that adsorption or elimination by different materials is easily realizable. The difference between these materials is due to their ability to fix pollutants and their elimination rates.

In this work, we will compare our results with those of some other authors, based on the removal rate and maximum retention capacity of acid green by different materials (Table 5).[46−54]

From this comparative study, it is clear that the removal of the AG1 dye by CLDH, which is total (100%), is much greater than that obtained with other materials. With a retention capacity of up to 833.33 mg/g, CLDH can be classified as having a relatively high retention capacity. This makes our material more efficient compared to other materials and promising for the adsorption and elimination of this pollutant.

2.9. Structural model

Before proposing an orientation of the anion AG1 between the layers, we determined the value of the length of the molecule AG1 via the molecular orbital semiempirical method with Gaussian 03 software; the calculated value for a horizontal position is 0.22 nm.

Figure 11 shows the orientation of AG1 dye intercalated between LDH sheets.

Table 5. Comparison of the removal rate and the acid green adsorption capacity of different adsorbent materials.

Materials	Dye	Q_m (mg/g)	Dye removal (%)	References
Lemna minor	Acid green 3	48.96	99.1	46
Rhodoturula glutinis biomass	Acid green 1	476.19	-	47
Cow dung ash	Acid green 20	176.99	-	
Mango stone ash	Acid green 20	242.72	-	48
Parthenium leaves ash	Acid green 20	684.93	-	
Activated carbon	Acid green 20	4.47	-	
Organo-bentonite	Acid green 25	2185.25	-	49
Polyaniline nanotubes	Acid green 25	6.896	-	50
Barley husk	Acid green 25	-	82.2	51
Chitosan	Acid green 9	138.89	99.3	52
Activated carbon	Acid green 25	182.6	94.2	53
Coconut husk	Acid green 25	46.6	93.2	54
CLDH	Acid green 1	833.33	100	This work
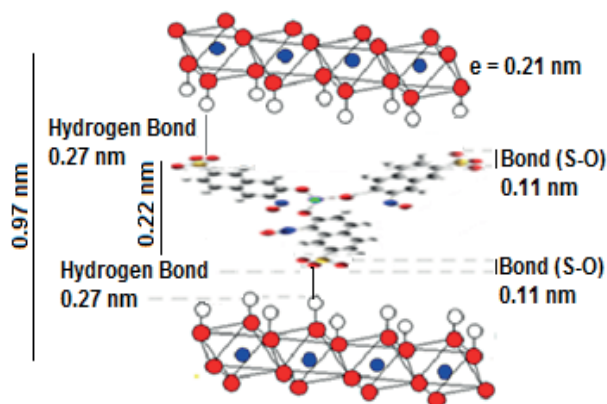
Figure 11. The schematic illustration of AG1 intercalation between brucitic sheets.

The interlamellar distance determined experimentally ($d = 0.98$ nm) suggests a horizontal direction (parallel to the layer planes) of the AG1 anion in the interlamellar space ($d = 0.11 + 0.11 + 0.27 + 0.27 + 0.21 = 0.97$–$0.98$ nm). The cohesion within the reconstructed material is ensured by hydrogen bonds between the dye sulfonate groups and the hydroxyl groups of the LDH sheets.

2.10. Recycling and regeneration of CLDH

The process for carrying out a cycle includes calcination, retention of polluting anions, and anion exchange with carbonates. Kovanda et al.[55] examined the possibility of removing arsenate, chromate, and vanadate anions in solution by CLDH [Mg_3-Al-CO_3] with its regeneration by repeating the same process. They mentioned that the retention capacity was reduced by 50% after the second cycle of calcination–rehydration. In another work concerning the decolorization of a textile effluent by CLDH, the authors reported a reduction in the decolorization capacity of 38% at the fifth cycle.[56]

The process involves five repeated cycles of calcination–rehydration–anion exchange with carbonates. Each cycle comprises the retention of the AG1 anion by calcined LDH at 500 °C, the anion exchange of AG1 anions retained by the carbonates in a Na_2CO_3 solution, and recalcination. The retention capacity of CLDH for the anion in each cycle is quantified using the Langmuir equation.

The retention capacities as a function of the number of cycles are represented in Figure 12. We note from these results that the five repeated cycles have no very significant effect on the retention capacity of the material.
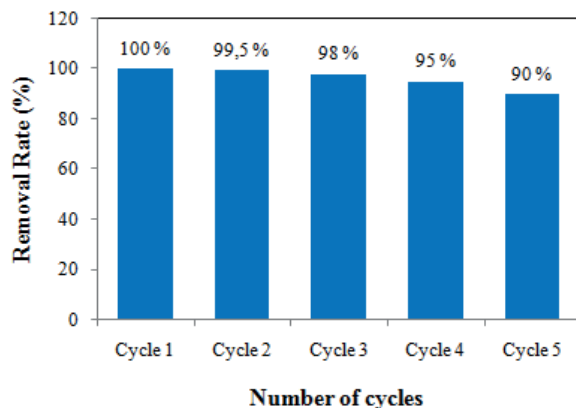

Figure 12. Variation of the elimination efficiency of the AG1 dye by CLDH as a function of number of cycles.

We can point out that, contrary to the results found by the authors cited above, the decrease in retention capacity is not very marked during the five repeated regeneration cycles; it is only reduced to 90% after the fifth cycle. This suggests that the retention capacity is influenced by the ability of CLDH to regenerate a lamellar structure during the rehydration process.

The AG1 removal rate is expressed by the following equation:

$$\% \text{ Removal Rate} = 100 \times (C_i - C_e) / C_i.$$

From the results of this work, it can be concluded that the material used has a relatively low cost and has proved very effective for the total removal of such pollutants (dyes). It can also be recycled by a series of anion exchange reactions of the dye retained by the carbonate anions, which will allow the recovery of pollutants and wash waters for possible reuse.

2.11. Conclusion

The kinetic study reflects a high affinity of CLDH material to the textile dye AG1. Equilibrium at room temperature is reached after 24 h. This is confirmed by kinetic modeling of the experimental data by the pseudo-second-order model.

The adsorption capacity depends on the initial pH of the solution. With a pH greater than 7 or less than 6, there is a decrease in the amount retained, respectively due to contamination with the carbonate ions and the partial dissolution of the matrix. However, maximum retention is obtained with an optimum pH between 6 and 7.

The comparative study of adsorption isotherms on a calcined phase and another uncalcined reveals that the former could be a good candidate for trapping such pollutants. The amount adsorbed of the textile dye depends on the mass ratio of AG1/CLDH.

The results of XRD and IR indicate that the retention is governed by adsorption textile dye on sites available on the surface of the reconstructed LDH phases ($[Zn_2$-Al-$CO_3]$ and $[Zn_2$-Al-AG1$]$) and by intercalation between the layers of the reconstructed LDH phase $[Zn_2$-Al-AG1$]$.

Rehydration of mixed oxides formed after calcination at 500 °C of the starting material in the presence of pollutants gives a reconstruction of the hydrotalcite phase with preservation of lamellar character (XRD, SEM).

The removal of dye in anionic form by CLDH gave satisfactory results. Under optimum conditions, the retention is total (100%) when the mass ratio of AG1/CLDH is between 0.58 and 0.75. The material can be recycled by a series of anion exchange reactions and its retention capacity reaches 833.33 mg/g. We also mention that this retention capacity was only reduced by 10% after the fifth recycling cycle.

3. Experimental

3.1. Preparation of $[Zn_2$-Al-$CO_3]$

The LDH compound (anionic clay) consists of brucitic sheets whose centers of octahedra are occupied by Zn and Al and the spaces between the sheets by the CO_3^{2-} anions and H_2O molecules. This material $[Zn_2$-Al-$CO_3]$ was synthesized reproducibly by coprecipitation method[57] at a constant pH of 10 with metal ratio Zn/Al = 2 and ripening time of 72 h under mild agitation, then calcined at a temperature of 500 °C for 5 h. $[Zn_2$-Al-$CO_3]$ was prepared starting from a mixture of metal salts solutions $Zn(SO_4)$, $7H_2O$ 0.4 M, and $AlCl_3$, $6H_2O$ 0.4 M, and a solution containing 0.3 M Na_2CO_3 and 0.1 M NaOH. At the beginning, some drops of the mixture of Na_2CO_3 and NaOH were added to 250 mL of distilled water to bring the pH back to the value of synthesis. The coprecipitation was performed by slow addition (2 mL/h) of a mixture of metal salts. The precipitate obtained was filtered, washed several times with distilled water, and then dried at room temperature (25 °C).

3.2. Retention experiments

The retention experiments were carried out at room temperature and under a stream of N_2 in order to avoid or at least minimize contamination by atmospheric CO_2. The initial pH of each solution was kept constant by addition of NaOH or HCl. The initial concentrations of AG1 ($C_{30}H_{15}FeN_3Na_3O_{15}S_3$, with a molecular weight of 878.46 g/mol) varied between 50 and 800 mg/L. Quantities of CLDH were dispersed in solutions of AG1 of 100 mL during well-defined times. After filtration, the obtained solid products were dried at room temperature before being analyzed by XRD, IR, and SEM. The supernatants were recovered and the residual dye concentrations were determined by UV-Vis spectroscopy. The absorbance was measured at 620 nm using a SPECTRONIC GENESYS 5 spectrophotometer (Thermo Fisher, Waltham, MA, USA).

The amount of AG1 retained by CLDH, Q (mg/g), was calculated as the difference between the initial and equilibrium (final) concentrations of the textile dye solution (C_i and C_e, respectively) by mass of the sorbent (m) in the volume of solution, V:

$$Q = (C_i - C_e)V/m.$$

3.3. Structural characterization techniques

The XRD equipment used was a Siemens D 501 diffractometer (Munich, Germany). Samples of unoriented powder were exposed to copper K_α radiation (λ = 0.15415 nm). Measurement conditions were 2 h, range

$5°–70°$, step size: 0.08–2 h, and step counting time: 4 s. Data acquisition was performed on a DACO-MP microcomputer. Unit cell constants were calculated using least squares refinement.

Absorbance IR spectra were recorded on a PerkinElmer 16 PC spectrophotometer (Waltham, MA, USA) at a resolution of 2 cm^{-1} and averaging over 100 scans, in the range of 400–4000 cm^{-1}. Samples were pressed into KBr disks.

SEM allows viewing the external morphology of materials. The principle of scanning is to scan the surface of the sample in successive rows and to transmit the sensor signal to a cathode ray tube whose scan is exactly synchronized with that of the incident beam. The scanning microscopes use a very fine beam, which scans the surface point by point of the sample. The analysis of the outer surface of the LDH was performed using a Philips device (Amsterdam, the Netherlands). The observations were carried out at a voltage of 5 kV.

References

1. Batzias, F. A.; Sidiras, D. K. *Bioresour. Technol.* **2007**, *98*, 1208-1217.

2. Tan, I. A. W.; Hameed, B. H.; Ahmed, A. L. *Chem. Eng. J.* **2007**, *127*, 111-119.

3. Ben Mansour, H.; Mosrati, R.; Corroler, D.; Bariller, D.; Ghedira, K.; Bariller, D.; Chekir-Ghedira, L. *Environ. Toxicol. Chem.* **2009**, *28*, 489-495.

4. Garg, V. K.; Amita, M.; Kumar, R.; Gupta, R. *Dyes Pigm.* **2004**, *63*, 243-250.

5. Macky, G.; Otterburn, M. S.; Sweeney, A. G. *Water Res.* **1980**, *14*, 15-20.

6. Robinson, T.; McMillan, G.; Marchant, R.; Nigam, P. *Bioresour. Technol.* **2001**, *77*, 247-255.

7. Auta, M.; Hameed, B. H. *Colloids Surf. B* **2013**, *105*, 199-206.

8. Nethaji, S.; Sivasamy, A.; Mandal, A. B. *Int. J. Environ. Sci. Technol.* **2013**, *10*, 231-242.

9. Chaari, I.; Feki, M.; Medhioub, M.; Bouzid, J.; Fakhfakh, E.; Jamoussi, F. *J. Hazard. Mater.* **2009**, *172*, 1623-1628.

10. Khaled, A.; El Nemr, A.; El-Sikaily, A.; Abdelwahab, O. *J. Hazard. Mater.* **2009**, *165*, 100-110.

11. Karaoğlu, M. H.; Doğan, M.; Alkan, M. *Desalination.* **2010**, *256*, 154-165.

12. Huang, R.; Liu, Q.; Huo, J.; Yang, B. *Arab. J. Chem.* **2017**, *10*, 24-32.

13. Bashi, A. M.; Hussein, M. Z.; Zainal, Z.; Rahmani, M.; Tichit, D. *Arab. J. Chem.* **2016**, *9*, 1457-1463.

14. Das, J.; Patra, B. S.; Baliarsingh, N.; Parida, K. M. *Appl. Clay Sci.* **2006**, *32*, 252-260.

15. Lv, L.; He, J.; Wei, M.; Evans, D. G.; Duan, X. *J. Hazard. Mater.* **2006**, *B133*, 119-128.

16. Ni, Z. M.; Xia, S. J.; Wang, L. G.; Xing, F. F.; Pan, G. X. *J. Colloid Interface Sci.* **2007**, *316*, 284-291.

17. Hosni, K.; Srasra, E. *Inorg. Mater.* **2008**, *44*, 742-749.

18. Crepaldi, E. L.; Tronto, J.; Cardoso, L. P.; Valim, J. B. *Colloid Surf. A* **2002**, *211*, 103-114.

19. Miyata, S. *Clays Clay Miner.* **1975**, *23*, 369-381.

20. Hashi, K.; Kikkawa, S.; Koizumi, M. *Clays Clay Miner.* **1983**, *31*, 152-154.

21. Mazeina, L.; Curtius, H.; Fachinger, J. *Clay Miner.* **2003**, *38*, 35-40.

22. Hibino, T.; Tsunashima, A. *Clays Clay Miner.* **1997**, *45*, 842-853.

23. Prasad, P. S. R.; Sarma, D. S.; Charan, S. N. *J. Geol. Soc. India* **2012**, *80*, 546-552.

24. Nakamoto, K. *Infrared Spectra of Inorganic and Coordination Compounds*; Wiley: New York, NY, USA, 1963.

25. Kameda, T.; Saito, M.; Umetsu Y. *Mater. Trans.* **2006**, *47*, 923-930.

26. Legrouri, A.; Lakraimi, M.; Barroug, A.; De Roy, A.; Besse, J. P. *Water Res.* **2005**, *39*, 3441-3448.

27. El Gaini, L.; Lakraimi, M.; Sebbar, E.; Meghea, A.; Bakasse, M. *J. Hazard. Mater.* **2009**, *161*, 627-632.

28. Elkhattabi, E.; Lakraimi, M.; Badreddine, M.; Legrouri, A.; Cherkaoui, O.; Berraho, M. *Appl. Water Sci.* **2013**, *3*, 431-438.

29. Ait Bentaleb, K.; El Khattabi, E.; Lakraimi, M.; Benaziz, L.; Sabbar, E.; Berraho, M.; Legrouri, A. *J. Mater. Environ. Sci.* **2016**, *7*, 2886-2896.

30. El Gaini, L.; Sebbar, E.; Boughaleb, Y.; Bakasse, M.; Lakraimi, M.; Meghea, A. *Nonlinear Optics Quantum Optics* **2007**, *00*, 1-13.

31. Ho, Y. S.; McKay, G. *Water Res.* **2000**, *34*, 735-742.

32. Okeola, F. O.; Odebunmi, E. O. *Adv. Nat. Appl. Sci.* **2010**, *4*, 281-288.

33. Cheung, W. H.; Szeto, Y. S.; McKay, G. *Technol.* **2007**, *98*, 2897-2904.

34. Kang, D. J.; Yu, X. L.; Tong, S. R.; Ge, M. F.; Zuo, J. C.; Cao, C. Y.; Song, W. G. *Chem. Eng. J.* **2013**, *228*, 731-740.

35. Yang, Y. Q.; Gao, N. Y.; Chu, W. H.; Zhang, Y. J.; Ma, Y. *J. Hazard. Mater.* **2012**, *209-210*, 318-325.

36. Choy, K. K.; Ko, D. C.; Cheung, C. W.; Porter, J. F.; McKay, G. *J. Colloid Interf. Sci.* **2004**, *271*, 284-295.

37. Ofomaja, A. E. *React. Funct. Polym.* **2010**, *70*, 879-889.

38. Özcan, A. S.; Erdem, B.; Özcan, A. *Colloid Surface A* **2005**, *266*, 73-81.

39. Zhang, X.; Huang, Q.; Liu, M.; Tian, J.; Zeng, G.; Li, Z.; Wang, K.; Zhang, Q.; Wan, Q.; Deng, F. et al. *Appl. Surf. Sci.* **2015**, *343*, 19-27.

40. Vimonses, V.; Jin, B.; Chow, C. W. K.; Saint, C. *J. Hazard. Mater.* **2009**, *171*, 941-947.

41. Bonnet, S.; Forano, C.; Besse, J. P. *Mater. Res. Bull.* **1998**, *35*, 783-788.

42. Prevot, V.; Forano, C.; Besse, J. P. *Inorg. Chem.* **1998**, *37*, 4293-4301.

43. Prevot, V.; Forano, C.; Besse, J. P. *Appl. Clay Sci.* **2001**, *18*, 3-15.

44. Ni, Z. M.; Xia, S. J.; Wang, L. G.; Xing, F. F.; Pan, G. X. *J. Colloid Interface Sci.* **2007**, *316*, 284-291.

45. Xie, Y.; He, C.; Liu, L.; Mao, L.; Wang, K., Huang, Q.; Liu, M.; Wan, Q.; Deng, F.; Huang, H. et al. *RSC. Adv.* **2015**, *5*, 82503-82512.

46. Balarak, D.; Mahdavi, Y.; Mostafapour, F. K.; Azarpira, H. J. *Chem. Mat. Res.* **2016**, *5*, 92-98.

47. Saravanan, P.; Princy, G.; Gandhi, N.; Renganathan, S. *Indian J. Environ. Prot.* **2012**, *32*, 207-214.

48. Purai, A.; Rattan, V. K. *Carbon Lett.* **2009**, *10*, 131-138.

49. Koswojo, R.; Utomo, R. P.; Ju, Y. H.; Ayucitra, A.; Soetaredjo, F. E.; Sunarso, J.; Ismadji, S. *Appl. Clay. Sci.* **2010**, *48*, 81-86.

50. Ayad, M. M.; Abu El-Nasr, A. *J. Nanostruct. Chem.* **2012**, *3*, 1-9.

51. Balarak, D.; Mostafapour, F. K.; Azarpira, H. *International Journal of Advanced Biotechnology and Research* **2016**, *7*, 1062-1070.

52. Asandei, D.; Dulman, V.; Todorciuc, T.; Bobu, E. *Cellulose Chem. Technol.* **2013**, *47*, 799-807.

53. Parimalam, R.; Raj, V.; Sivakumar, P. *J. Chem.* **2012**, *9*, 1683-1698.

54. Abdul Halim, H. N.; Yatim, N. S. M. In *Proceedings of the International Conference on Environment and Industrial Innovation IPCBEE*; IACSIT Press: Singapore, 2011, pp. 268-272.

55. Kovanda F.; Kovacsova E.; Kolousek D. *Collect. Czech. Chem. Commun.* **1999**, *64*, 1517-1528.

56. Teixeira, T. P. F.; Aquino, S. F.; Pereira, S. I.; Dias, A. *J. Chem. Eng.* **2014**, *31*, 19-26.

57. Miyata, S. *Clays Clay Miner.* **1983**, *31*, 305-311.